Novel geopolymer for use as a sensible storage option in high temperature thermal energy storage systems

Cite as: AIP Conference Proceedings **2303**, 190019 (2020); https://doi.org/10.1063/5.0028721
Published Online: 11 December 2020

Rhys Jacob, Neil Trout, Aran Solé, et al.

Novel Geopolymer for Use as a Sensible Storage Option in High Temperature Thermal Energy Storage Systems

Rhys Jacob[1a], Neil Trout[2], Aran Solé[3], Stephen Clarke[2], A. Inés Fernández[4], Luisa F. Cabeza[5], Wasim Saman[1], Frank Bruno[1]

[1] *Future Industries Institute, University of South Australia, Mawson Lakes, SA 5095, Australia*
[2] *Care of Our Environment, Adelaide, SA 5000, Australia*
[3] *Department of Mechanical Engineering and Construction, Universitat Jaume I, Campus del Riu Sec s/n, 12071 Castelló de la Plana, Spain*
[4] *Department of Materials Science and Physical Chemistry, Universitat de Barcelona, Martí i Franqués 1, 08028 Barcelona, Spain*
[5] *GREA Innovació concurrent, INSPIRES Research Centre, University of Lleida, Pere de Cabrera s/n, 25001, Lleida, Spain*

[a)] Corresponding author: rhys.jacob@unisa.edu.au

Abstract. In the current study a novel geopolymer created from waste materials (namely fly ash and black slag) has been characterised as a potential high temperature thermal energy storage material option. Several geopolymer samples have been fabricated and characterised by X-ray diffraction (XRD) and scanning electron microscopy (SEM). Additionally, the density and heat capacity have been determined. Lastly, the cost of the material and packed bed system was estimated showing that the geopolymer-based systems are potentially 35% cheaper than the traditional 2-tank molten salt systems.

NOMENCLATURE

Symbol	Definition	Unit	Symbol	Definition	Unit
A	*Area under DSC curve*	-	C	*Cost*	$
Cp	*Specific Heat Capacity*	kJ/kg·K	H	*Height*	m
M	*Mass*	kg	Q	*Energy*	kJ
r	*Radius*	m	V	*Volume*	m^3
w	*Wall thickness*	m	ε	*Porosity*	-
ρ	*Density*	kg/m^3	ΔT	*Temperature Difference*	°C

Subscript	Definition	Subscript	Definition	Subscript	Definition
F	*Foundation*	f	*Fluid*	I	*Insulation*
m	*Solid material*	s	*Sapphire*	t	*Tank*
tm	*Tank material*				

INTRODUCTION

High temperature thermal energy storage (TES) is an important technology for minimising energy loss for industrial waste heat recovery applications and compressed air energy storage (CAES) systems.

SolarPACES 2019
AIP Conf. Proc. 2303, 190019-1–190019-11; https://doi.org/10.1063/5.0028721
Published by AIP Publishing. 978-0-7354-4037-1/$30.00

It can also be used to extend the operational times of renewable energy power systems such as concentrated solar power (CSP). For the industrial sector, 43% of heat required is greater than 400°C [1] while it is estimated that between 20% and 50% of the industrial energy input is lost as waste heat between 120°C and 1,700°C, totaling 440 TWh in the United States alone [2]. The benefits for CSP are similar, with studies showing the installation of 12 hours of full storage capacity can lower the levelised cost of energy (LCOE) by 10% [3]. Although the economic and environmental benefits of this type of technology are many, uptake of TES for these applications has been slow. The reason for this is the general high cost of commercially available systems [4] and the large environmental impact of the traditional two-tank molten salt systems [4-5]. Despite being adopted in a third of all CSP plants [6], the current state-of-the-art two-tank molten salt has several important limitations moving forward. These limitations include a high cost of the system [7, 8], a high freezing point (220°C) which requires expensive freeze-protection of pipes and tanks, and a maximum operating temperature of 565°C. Therefore, for high temperature TES to be more widely adopted, a storage material must be identified which is economically viable, abundant and readily available, environmentally friendly, stable at desirable operating temperatures (300-900°C) and possess desirable physical and thermophysical properties (high heat capacity, material compatibility, etc.) The valorisation of industrial by-products [9] or usage of abundant materials is a suitable approach to solve this issue as these materials are both cost effective and have a low environmental impact. To this end several options have been proposed such as treated asbestos waste (Cofalit©) [10], fly ash-based products [11], electric arc furnace (EAF) slag [12], and desert sand [13].

An alternative to these materials would be the use of geopolymers fabricated with the use of industrial waste products such as fly ash and black slag. Fly ash is used as a replacement of ordinary Portland cement (OPC) to reduce the cost and environmental impact of concrete. In addition to this, fly ash-based concrete can be tailored to exhibit a higher compressive strength, greater resistance to aggressive environments, increased workability or a greater resistance to high temperatures than traditional concrete [14]. Fly ash production in the US was estimated to be 48.4 million tonnes in 2013 and forecast to increase to 49.5 million tonnes in 2033 [15]. Meanwhile the utilisation of fly ash was 44% in 2013 and predicted to rise to 65% in 2033 [15]. Even if this goal is reached, over 450 million tonnes of fly ash will be landfilled in this time. With landfill area becoming increasingly sparse, the reuse of fly ash becomes an important factor.

To this end a novel geopolymer has been fabricated using recycled materials for use as a potential high temperature sensible storage option. The implementation of the proposed geopolymer is for a packed-bed thermocline storage design. This design has shown good reliability and lower costs, with a commercial packed-bed system being operated in conjunction with a CSP plant in Morocco [16]. In the current study the physical, thermophysical, and structural characterisation of the novel geopolymer have been performed. In addition, the applicability of this material in the context of high temperature TES is investigated by considering the material compatibility and durability, as well as the cost of a utility scale potential system. These results are then compared to other studied materials.

METHOD

A previous investigation into geopolymers fabricated with various materials was undertaken in [17]. From this study a geopolymer consisting of 50:50 wt% fly ash and black slag warranted further investigation and is explored in the current study.

Materials

Geoploymer Samples

In the current study a novel geopolymer consisting of 50% fly ash and 50% black slag with sodium silicate solution as a binder was fabricated. The fly ash was sourced from Hallett Concrete and Resources (South Australia), while the black slag was sourced from Nyrstar Port Pirie which then had to be ground so that it could form the geopolymer. The sodium silicate solution was purchased from Sigma Aldrich at reagent grade (37.1% $Na_2O(SiO_2)x$). The fly ash and black slag was mixed with the sodium silicate solution at a ratio of 15:15:13 to form a thick paste. To achieve a solid material, the sample was cured for 7 days at room temperature. It was then left for 3 days at 80°C and finally fired at 200°C for 4 days [18] (*Fig. 1*).

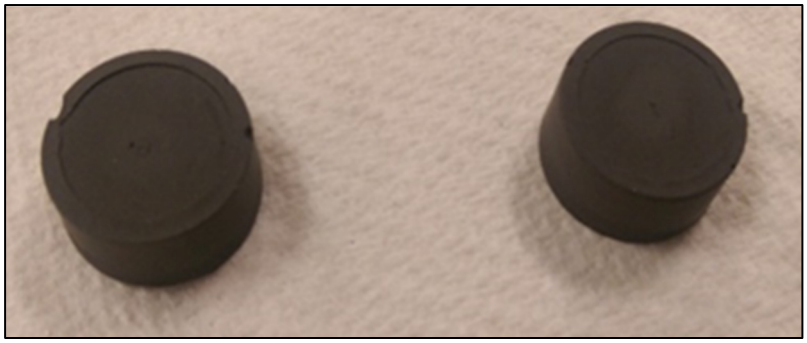

FIGURE 1. Prepared Geopolymer Samples

Heat Capacity

A Mettler-Toledo 822e DSC was used to characterize the specific heat capacity (Cp) of the geopolymer. The Cp has been determined by the areas method, which consists of consecutive isothermal segments with no heating stages amid, obtaining a peak for each variation of 1ºC temperature between the isotherms. The same temperature program is performed for the sapphire reference material, and the material under study. Then, the specific heat capacity of the material can be calculated using *Equation 1* [19]:

$$Cp_m = \frac{Cp_s \cdot A_m}{A_s} \quad (1)$$

where As (J/g) is the integrated peak area for the sapphire curve, Am (J/g) is the integrated peak area for the material curve, Cps (J/g·ºC) is the sapphire specific heat capacity and Cpm (J/g·ºC) is the material specific heat capacity. The sapphire specific heat capacity can either be found in the literature or obtained by the Mettler-Toledo software. Thus, all the required parameters are known. The temperature program was set from 100 to 450ºC, according to the application, with three steps of 1ºC from 100 to 101ºC, from 300 to 301ºC, and from 449 to 450ºC, applying a heating rate of 15 K/min between steps, to obtain the Cp at these three different temperatures. Two samples of the geopolymer and two consecutive DSC analyses were performed for both samples to ensure repeatability of the results.

XRD Analysis

XRD analysis was performed with powder samples to characterise crystalline phases. The analysis was carried out in a Bragg–Brentano Siemens D-500 powder diffractometer device with CuKα radiation. The identification of all phases was made with X'Pert HighScore software and PDF-2 2006 database.

Density

The density of the uncycled geopolymer was measured using the Archimedes principle using water as the test fluid and found to be 2,592 kg/m^3.

RESULTS AND DISCUSSION

Thermophysical Properties

Heat Capacity

By analysing the DSC curves using the methodology described above, the sample heat capacity values for a range of temperatures could be found (*Fig. 2*).

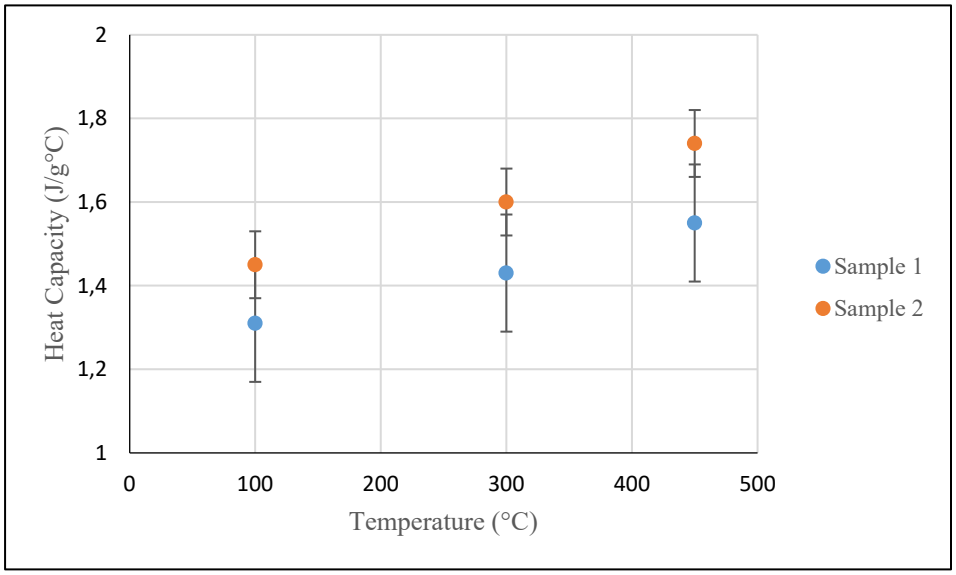

FIGURE 2. Experimental Heat Capacity Values of Geopolymer Samples

Figure 2 shows that the results are in agreement and a common pattern can be observed. Using the experimental data obtained, a linear estimation of heat capacity with temperature can be established (*Equation 2*).

$$Cp_m = 0.00075T + 1.3 \pm 0.11 \quad (2)$$

The developed material has a very promising heat capacity which makes it a viable material for sensible heat storage applications. This is further discussed in the *'Economic Viability'* section below.

Thermal Conductivity

The thermal conductivity of coal fly ash and solid black slag has been studied in the past and is estimated to be 1-1.7 W/m·K [9], while the estimated thermal conductivity of the coal fly ash is between 1.3-2.1 W/m·K [11]. Using this information, the expected thermal conductivity of the geopolymer samples is between 1.2-1.9 W/m·K between 100-900°C.

Particle Size and Distribution

To witness the porosity and particle distribution in the geopolymer sample, micrographs of this sample (50%FA/50%BS) at a range of magnifications are shown in *Fig. 3-4*.

The micrographs in *Fig. 3-4* show the structure of the geopolymer. At 200µm the porosity of the sample can be clearly seen (the black areas in *Fig. 3-4*). The larger areas of void have been identified as areas where particles have been dislodged (possibly during the preparation process) and would not be present throughout the sample.

The difference in particle size and shape can also be identified with the finer particles (dark grey areas in *Fig. 3-4* being identified as the fly ash while the larger geometric particles being identified as coming from the black slag.

Interestingly there also appears a large spherical particle which is thought to be from the fly ash at a much higher size than originally sourced. At 100 µm the difference in the particles can be more clearly seen with areas previously identified as void actually being fly ash particles. At 50 µm the boundary of void/black slag/fly ash is clearly identifiable. It can also be seen that some of the black slag particles appear to have a 'white' glow suggesting that there may be a coating on the surface (possibly from the sodium silicate binder).

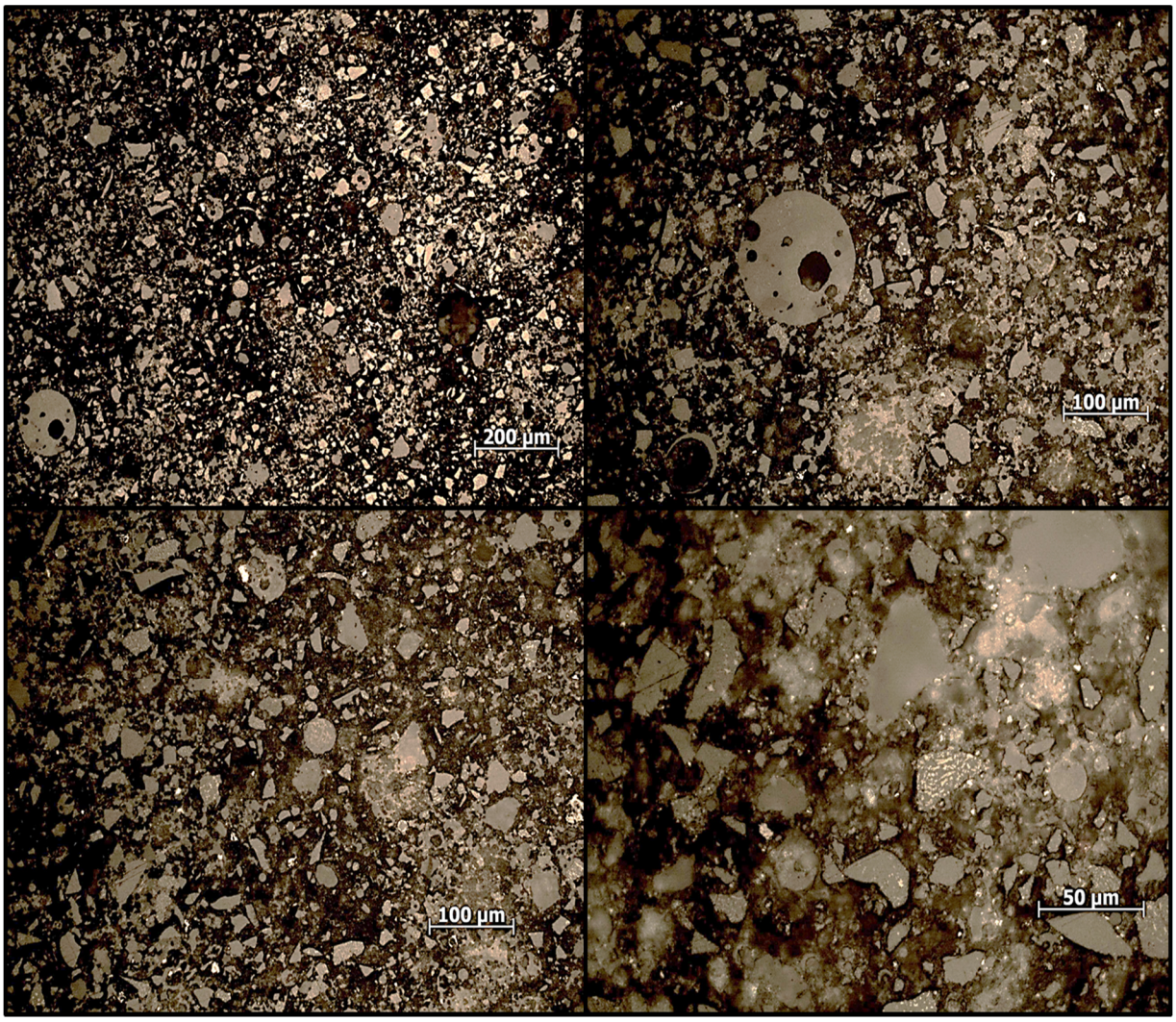

FIGURE 3. Micrographs of Geopolymer Sample

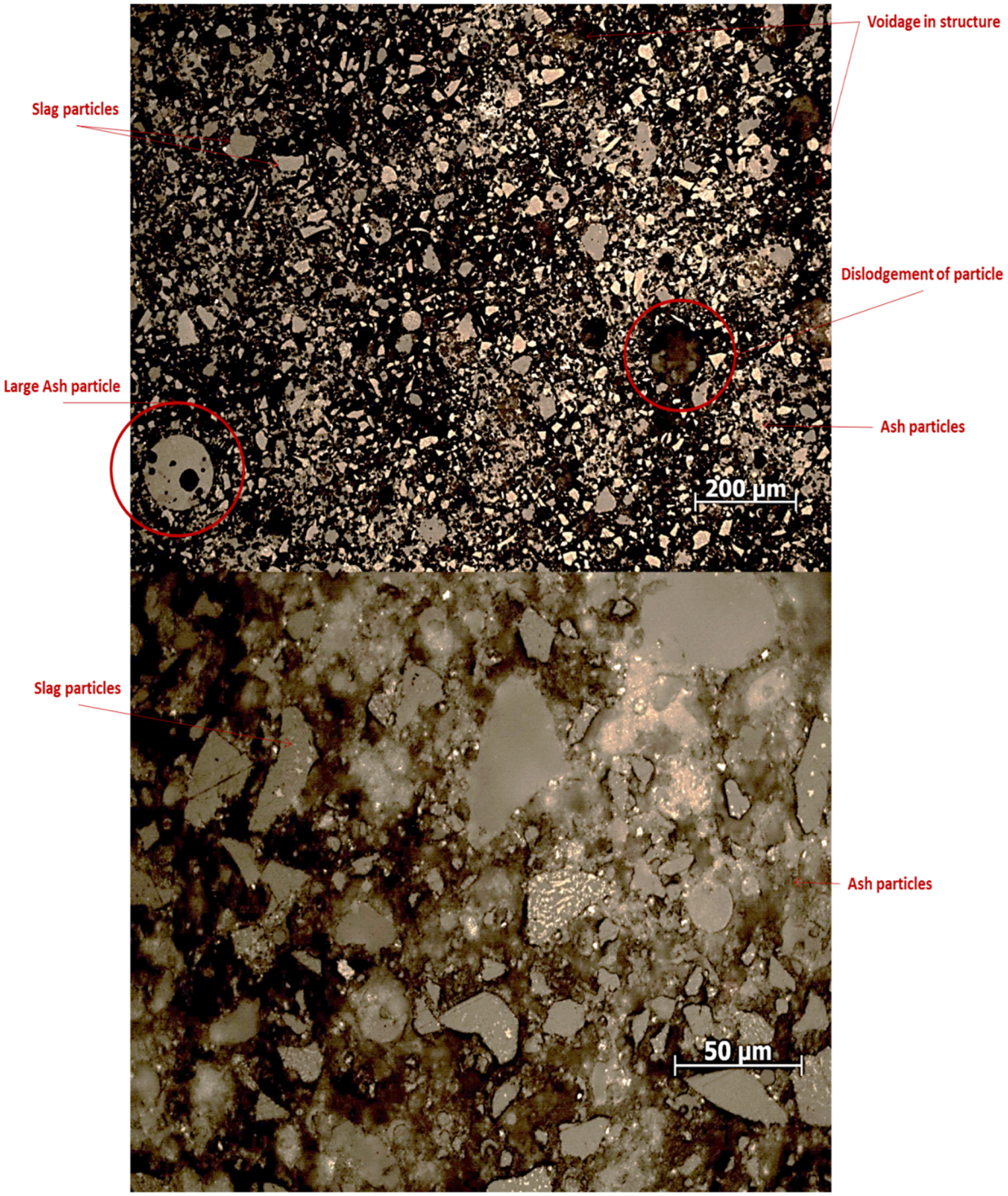

FIGURE 4. Micrographs of Geopolymer showing Ash and Slag Particles

Analysis of Crystalline Phases

The structural analysis of the geopolymer sample was completed using XRD analysis, the results of which can be seen in *Fig. 5*. As can be seen from *Fig. 5a* there is a clearly identifiable trend in the XRD spectra which is indicative of a largely amorphous material. Furthermore, *Fig. 5b* shows the likely phases present in the geopolymer sample.

Silicon oxide in the form of Quartz is a major component of the crystalline part of the materials, as well as iron oxide in the form of Wuestite and Hermatite. Also, as expected for the sample, alumina silicate is present as Mullite.

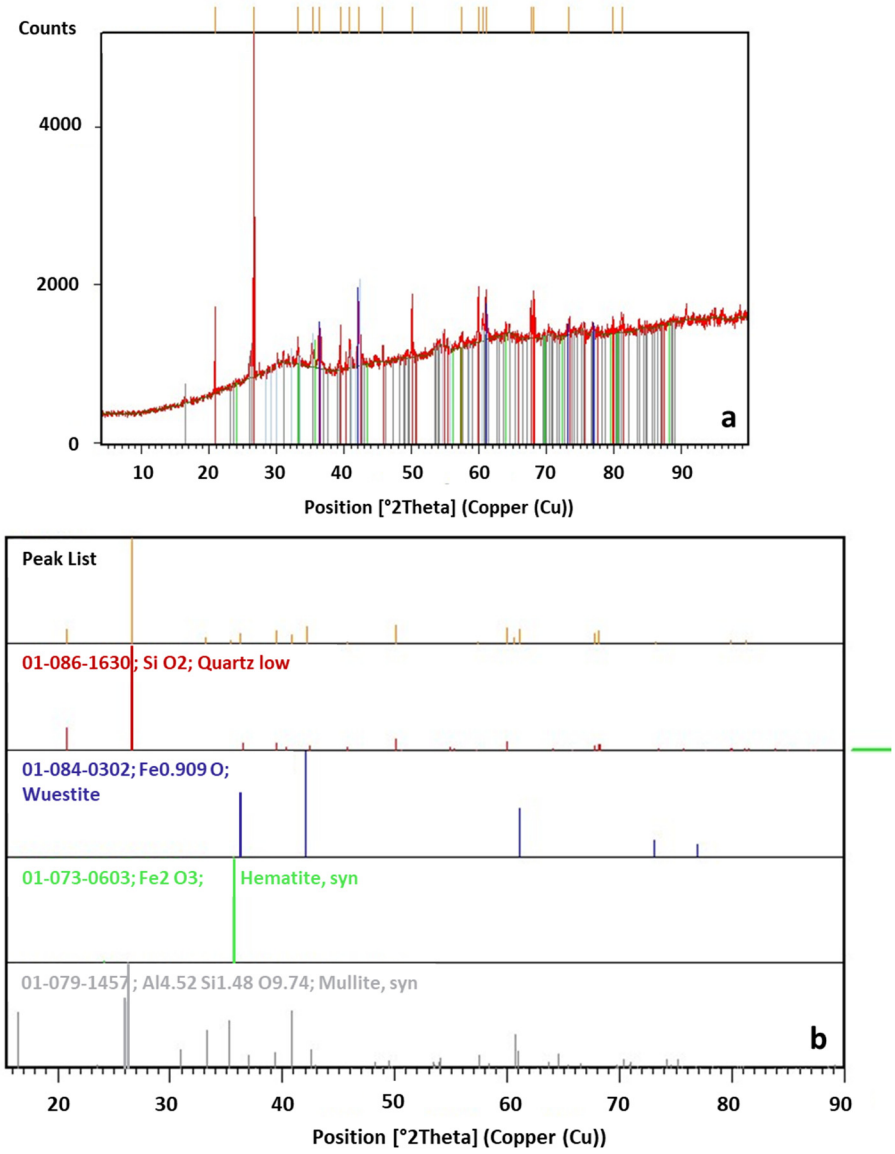

FIGURE 5. XRD Analysis for Geopolymer Sample
a) XRD Spectra; b) Identified Phases

ECONOMIC VIABILITY

The economic viability of the studied geopolymer as a high temperature TES option was determined by investigating the cost of the material, the CAPEX of a potential TES system utilising the proposed geopolymer, and a techno-economic comparison with other potential filler materials.

Material Cost

The cost of the material is an important factor to consider when evaluating storage systems as it can make up a large portion of the total system cost. To calculate the estimated cost of the geopolymer filler, bulk prices were found for the raw materials (*Table 1*). As the process of making the geopolymer is fairly simple and can be done using existing technology, no additional processing cost was applied.

TABLE 1. Raw Material Bulk Cost

Material	Price (USD/kg)	Reference
Fly Ash Powder	0.04	[20]
Black Slag Powder	0.04*	[20]
Sodium Silicate Solution	0.15	[21]
TOTAL	0.07	

** Assumed to be the same as Fly Ash*

Therefore, it was found that the estimated cost of the geopolymer filler will be approximately US $0.07/kg.

CAPEX Estimation

For the CAPEX estimate of a sensible system, it is important to consider the storage material and the storage container. Therefore, in the following example, a 10 MWh_t system is designed and the CAPEX estimated for a system utilising the proposed geopolymer as the solid filler and air as the storage fluid. *Table 2* shows some of the important parameters used to estimate the size of the system and therefore the cost. Because of the high operational temperatures expected in such a system, stainless steel 316 (SS316) was chosen as the tank material.

TABLE 2. Storage System Parameters

Material	Parameter	Value	Material	Parameter	Value
Geopolymer	Density (kg/m^3) [ρ_s]	*2,592*	Tank	Aspect Ratio (r:H)	*1:1*
Geopolymer	Heat Capacity (kJ/kgK) [Cp_s]	*1.6*	Tank	Wall Thickness (m) [w_t]	*0.039*
Geopolymer	Cost ($/kg)	*0.07*	SS316	Density (kg/m^3) [ρ_t]	*7,900*
Air	Density (kg/m^3) [ρ_f]	*0.5*	SS316	Cost (USD/kg) [C_{ss}]	*3.28* [22]
Air	Heat Capacity (kJ/kgK) [Cp_f]	*1.07*	Insulation	Cost ($/m^2) [$C_I$]	*235*
Air	Cost ($/kg)	-	Foundation	Cost ($/m^2) [$C_F$]	*1,210*
Tank	Porosity [ε]	*0.28*	Tank	Radius (m) [r_t]	*2.74*
System	Effectiveness (%)	*69*	System	Temperature Difference (°*C*)	*270*

To estimate the tank volume required to achieve the desired storage capacity *Equation 3* can be used. The tank dimensions can also be calculated using *Equation 4*. The storage efficiency is set at 69% in line with thermocline systems presented in [23].

$$V_t = \frac{Q}{((\rho_m * Cp_m * \Delta T * \varepsilon) + (\rho_f * Cp_f * \Delta T * (1-\varepsilon))} \quad (3)$$

$$r_t = \frac{V_t}{(\pi)^{\frac{1}{3}}} \quad (4)$$

Using the tank aspect ratio, (1:1), the tank height can also be calculated. Furthermore, the mass required of the storage fluid and storage filler can now be calculated.

$$M_m = V_t * \rho_m * (1 - \varepsilon) \quad (5)$$

$$M_f = V_t * \rho_f * \varepsilon \quad (6)$$

With the tank dimensions and storage mass known, the cost of the system can be estimated. Using previous estimates from [3, 24-26], the cost of the tank can be calculated while the cost of the storage material can be estimated using the bulk prices of the material (*Equation 7*).

$$C_t = (\rho_t * H_t(\pi((r_t + w_t)^2 - r_t^2) * C_{tm}) + (\pi * (r_t + w_t)^2 * C_I) + (2 * \pi * (r_t + w_t) * H_t * C_F) \quad (7)$$

Construction, engineering and inspection, and contingency costs are added as 30%, 20% and 7%, respectively, of the total direct cost. It was found for the studied system that the cost of the system is \$16.21/kWh$_t$, which is much lower than published 2-tank molten salt costs (24-26 \$/kWh$_t$) [7-8], traditional sensible systems (19-30 \$/kWh) [7-8], and 1-PCM EPCM systems (21-22 \$/kWh$_t$) [7]. The cost reported in the current study is also comparable with hybrid multi-layer sensible/PCM systems (14.5-16.5 \$/kWh$_t$) [8] presenting a good option for optimisation and hybridisation to further reduce costs.

Comparison to Other Sensible Options

To assess the techno-economic viability of the proposed geopolymer filler, a comparison with other potential sensible fillers was performed (*Table 3*).

TABLE 3. Comparison of Various Sensible Storage Options

Material	Density (kg/m^3)	Heat Capacity (kJ/kg·K)	Cost (USD/kg) ^	Energy Density (kJ/m^3)*	Cost of Energy Density (kJ/USD)*	REF
Geopolymer	2,592	1.6	0.07	1,119,744	6,171	*Current Study*
Alumina	3,953	1.16	0.35	1,238,080	895	[12]
Rock/Quartz	2,500	0.83	0.2	560,250	1,121	[27]
Silicon Carbide	3,210	0.75	1.03	650,025	197	[17]
Castable Ceramic	3,500	1.35	5	1,275,750	73	[12]
Cofalit®	3,120	0.86	0.01	724,464	23,220	[12]
EAF Slag 1	3,430	0.93	0.09	861,273	2,790	[12]
EAF Slag 2	3,770	0.91	0.09	926,289	2,730	[12]
Solar Salt	1,870	1.6	0.69	807,840	626	[12]
WBA	2,586	0.29	0.0006	202,473	130,500	[28]
Magnetite	5,150	1.1	0.18	1,529,550	1,650	[29]

**Based on a ΔT=270°C*

^ Costs indicated are for raw material only. Does not include any further processing etc. that may be required.

From *Table 3* it can be seen that the geopolymer compares well with other commonly used materials such as solar salt and quartzite. Furthermore, it compares favourably with other waste-based materials such as EAF slag but is slightly more costly than the presented values of Cofalit® and WBA. One of the disadvantages of this material is the physical density which is much lower than other ceramics and solids.

This may lead to large storage containment vessels but is largely offset by its superior heat capacity and low cost. Therefore, this material presents an attractive option as an alternative to commonly used materials or ceramic-based alternatives.

CONCLUSIONS

In the current study a novel geopolymer created from waste materials (namely fly ash and black slag) has been characterised as a potential high temperature thermal energy storage option. The geopolymer can be easily shaped and cured at low temperatures facilitating a range of structure shapes while minimising processing costs. Samples of the geopolymer underwent several characterisation tests including heat capacity and density. The heat capacity of the sample was found to increase from 1.38 kJ/kg·K at 100°C, to 1.64 at 450°C, indicating excellent specific heat. The density of the uncycled geopolymer was found to be 2,592 kg/m^3. Lastly, an economic analysis has shown that a packed bed with geopolymer filler is approximately 35%, 30%, and 23% cheaper than the traditional molten salt 2-tank, traditional sensible, and single PCM systems, respectively. It also compares very well with other potential filler materials showing that the geopolymer filler can be a viable option for high temperature TES.

ACKNOWLEDGEMENTS

This research was performed as part of the Australian Solar Thermal Research Institute (ASTRI), a project supported by the Australian Government, through the Australian Renewable Energy Agency (ARENA).

The work was partially funded by the Spanish government (ENE2015-64117-C5-1-R (MINECO/FEDER)). The authors would like to thank the Catalan Government for the quality accreditation given to their research group (2014 SGR 123). GREA is certified agent TECNIO in the category of technology developers from the Government of Catalonia. This project has received funding from the European Commission Seventh Framework Programme (FP/2007-2013) under Grant agreement Nº PIRSES-GA-2013-610692 (INNOSTORAGE) and from the European Union's Horizon 2020 research and innovation programme under grant agreement No 657466 (INPATH-TES). Aran Solé would like to thank Ministerio de Economía y Competitividad de España for Grant Juan de la Cierva, FJCI-2015-25741. The authors would also like to acknowldege the Diopma group from the University of Barcelona thanks the funding by the Spanish Government (RTI2018-093849-B-C32), and the Catalan Government for the quality accreditation (2017 SGR 118).

REFERENCES

1. Industrial Solar (2016). Available at: http://www.industrial-solar.de/CMS/en/solutions/solare-prozesswaerme/ [Last Accessed: 15th March, 2016]
2. US Department of Energy (2008). *Waste heat recovery: technology opportunities in the US industry*. Tech. Rep.
3. Herrmann U, Kelly B, Price H. Energy (2004); **1**(29): 883-893.
4. Jacob R, Belusko M, Inés Fernández A, Cabeza L.F, Saman W, Bruno F. Applied Energy (2016); **180**: 586–597.
5. Miró L, Oró E, Boer D, Cabeza L.F. Applied Energy (2015); **137**: 793–799.
6. NREL (2016). *Concentrating Solar Power Projects*. Available at: http://www.nrel.gov/csp/solarpaces/ [Last Accessed: 15th March, 2016]
7. Xu B, Li P, Chan C. Applied Energy (2015); **160**: 286–307.
8. Zhao B-c, Cheng M-s, Liu C, Dai Z-m. Applied Energy (2016); **178**: 784–799.
9. Gutierrez A, Miró L, Gil A, Rodríguez-Aseguinolaza J, Barrenche C, Calvet N, Py X, Inés Fernández A, Grágeda M, Ushak S, Cabeza L.F. Renewable and Sustainable Reviews (2016); **59**: 763-783.
10. Calvet N, Gomez J, Faik A, Roddatis V, Meffre A, Glatzmaier G, Doppiu S, Py X. Applied Energy (2013); **109**: 387–393.
11. Meffre A, Py X, Olives R, Bessada C, Veron E, Echegut P. Waste Biomass Valor (2015); **6**: 1003–1014.
12. Ortega-Fernandez I, Calvet N, Gil A, Rodríguez-Aseguinolaza J, Faik A, D'Aguanno B. Energy (2015); **89**: 601-609.
13. Diago M, Crespo Iniesta A, Delclos T, Shamim T, Calvet N. Energy Procedia (2015); **75**: 2113 – 2118. Proceedings of The 7th International Conference on Applied Energy – ICAE2015.
14. Al Bakri MM, Mohammed H, Kamarudin H, Khairul Niza I, Zarina Y. Journal of Engineering and Technology Research (2011); **3**(1): 1-4.

15. American Coal Ash Association (ACCA) (2015). *Key Findings 2015-Coal Combustion Products Utilization-U.S. Historical Perspective and Forecast*. Available at: https://www.acaa-usa.org/Portals/9/Files/PDFs/Key-Findings-Report-2015.pdf
16. Airlight Energy (2016). *Concentrated Solar Power*. Available at: http://www.airlightenergy.com/csp/. [Last Accessed 1st March, 2016]
17. Jacob R, Trout N, Raud R, Clarke S, Steinberg T.A, Saman W, Bruno F. AIP Conference Proceedings **1734**, 050021 (2016); doi: 10.1063/1.4949119.
18. Jacob R, Raud R, Trout N, Bell S, Clarke S, Will G, Saman W, Bruno F. Solar Energy Materials and Solar Cells (2018); **174**: 271–276.
19. Ferrer G, Barreneche C, Solé A, Martorell I, Cabeza LF. Journal of Energy Storage (2017); **11**: 1-6.
20. Alibaba (2016). *Fly Ash*. Available at: http://www.alibaba.com/product-detail/Good-Price-Dry-Fly-Ash-for_60343784409.html?spm=a2700.7724838.0.0.Dgt85q
21. Alibaba (2016). *Sodium Silicate Solution*. Available at: http://www.alibaba.com/product-detail/water-glass-sodium-silicate-Solution-silicate_1823687911.html?spm=a2700.7724857.29.48.u4pHRb
22. MEPS (December, 2016). *World Stainless Steel Prices- 316 Hot Rolled Plate*. Available at: http://www.meps.co.uk/Stainless%20Prices.htm
23. Brosseau D, Hlava P, Kelly M, (2004). Testing Thermocline Filler Materials and MoltenSalt Heat Transfer Fluids for Thermal Energy Storage Systems Used in Parabolic Trough Solar Power Plants. Sandia National Labratories, SAND2004-3207. Available at: http://www.nrel.gov/csp/troughnet/pdfs/brosseau_sand2004_3207_final.pdf
24. Nithyanandam K, Pitchumani R. Solar Energy (2014); **107**: 770–788.
25. Kelly B, Kearney D, (2006). *Thermal storage commercial plant design for a 2-tank indirect molten salt system*. National Renewable Energy Laboratory, NREL/SR-550040166, pp. 1–32.
26. Jacob R, Belusko M, Saman W, Bruno F. *Economic Studies on High-Temperature Phase Change Storage Systems*. High Temperature Thermal Storage Systems using Phase Change Materials. **Ed:** N.H.S Tay and L. F. Cabeza (2018). Elsevier, London.
27. Galione P.A, Pérez-Segarra C.D, Rodríguez I, Oliva A, Rigola J. Applied Energy (2015); 142: 337–351.
28. del Valle-Zermeño R, Barreneche C, Cabeza L.F, Formosa J, A. Inés Fernández, Chimenos J. Renewable Energy (2016); **99**: 431-436.
29. Grosu Y, Faik A, Ortega-Fernández I, D'Aguanno B. Solar Energy Materials & Solar Cells (2017); **161**: 170–176.